

Broken symmetry, excitons, gapless modes and topological excitations in Trilayer Quantum Hall systems

Jinwu Ye

Department of Physics, The Pennsylvania State University, University Park, PA, 16802

(March 22, 2022)

We study the interlayer coherent incompressible phase in Trilayer Quantum Hall systems (TLQH) at total filling factor $\nu_T = 1$ from three approaches: Mutual Composite Fermion (MCF), Composite Boson (CB) and wavefunction approach. Just like in Bilayer Quantum Hall system, CB approach is superior than MCF approach in studying TLQH with broken symmetry. The Hall and Hall drag resistivities are found to be quantized at h/e^2 . Two neutral gapless modes with linear dispersion relations are identified and the ratio of the two velocities is close to $\sqrt{3}$. The novel excitation spectra are classified into two classes: Charge neutral bosonic 2-body bound states and Charge ± 1 fermionic 3-body bound states. In general, there are two 2-body Kosterlize-Thouless (KT) transition temperatures and one 3-body KT transition. The Charge ± 1 3-body fermionic bound states may be the main dissipation source of transport measurements. The broken symmetry in terms of $SU(3)$ algebra is studied. The structure of excitons and their flowing patterns are given. The coupling between the two Goldstone modes may lead to the broadening in the zero-bias peak in the interlayer correlated tunnelings of the TLQH. Several interesting features unique to TLQH are outlined. Limitations of the CB approach are also pointed out.

I. INTRODUCTION

Quantum Hall Effect (FQHE) in multicomponent systems has attracted a lot of attention since the seminal work by Halperin [1]. These components could be the spins of electrons when the Zeeman coupling is very small or layer indices in multi-layered system. In particular, spin-polarized Bilayer Quantum Hall (BLQH) systems at total filling factor $\nu_T = 1$ have been under enormous experimental [2–5] and theoretical [6–13] investigations over the last decade. When the interlayer separation d is sufficiently large, the bilayer system decouples into two separate compressible $\nu = 1/2$ layers. However, when d is sufficiently small, in the absence of interlayer tunneling, the system undergoes a quantum phase transition into a novel spontaneous interlayer coherent incompressible phase [11].

By treating the two layer indices as two pseudo-spin indices, Girvin, Macdonald and collaborators [9–11] mapped the bilayer system into a Easy Plane Quantum Ferromagnet (EPQFM). They achieved the mapping by projecting the Hamiltonian of the BLQH onto the Lowest Landau Level (LLL) and then using subsequent Hartree-Fock (HF) approximation and gradient expansion (called LLL+HF in the following). They explored many rich and interesting physical phenomena in this system. The low energy excitations above the ground state is given by an effective $2+1$ dimensional XY model. In addition to the Goldstone mode, there are also 4 flavors of topological defects called "merons" which carry fractional charges $\pm 1/2$ and also have \pm vorticity. They have logarithmic divergent self energies and are bound into pairs at low temperature. The lowest energy excitations carry charge $\pm e$ which are a meron pair with opposite vorticity and the same charge. There is a finite tempera-

ture Kosterlize-Thouless (KT) phase transition at T_{KT} where bound states of the 4 flavors of merons are broken into free merons. Unfortunately, this transition has not been observed so far. The EPQFM approach is a microscopic one which takes care of LLL projection from the very beginning. However, the charge sector was explicitly projected out, the connection and coupling between the charge sector which displays Fractional Quantum Hall effect and the spin sector which displays interlayer phase coherence was not obvious in the EPQFM approach.

In [12], I used and extended both Mutual Composite Fermion (MCF) and Composite Boson (CB) approaches to study both balanced and imbalanced BLQH and made critical comparisons between the two approaches. I identified several serious problems with the MCF approach and then developed a simple CB approach which naturally avoids all these problems suffered in the MCF approach. I found the CB approach is superior to MCF approach in the BLQH with broken symmetry. The functional form of the spin sector of the CB theory is the same as the EPQFM. It also has the advantage to treat charged excitations and the collective order parameter fluctuations in the pseudo-spin sector on the same footing, therefore can spell out the spin-charge connections explicitly. From this spin-charge connection, we are able to classify all the possible excitations in the BLQH in a systematic way. The CB theory may also be applied to study the incoherent disordered insulating side and the quantum phase transitions between different ground states [13]. Using the CB approach, I also studied several interesting phenomena specific to im-balanced BLQH. Just like any Chern-Simon theory, the CB theory in BLQH has its own limitations: it is hard to incorporate the LLL projection (see however [14]), some parameters can only be taken as phenomenological parameters to be fitted into the micro-

scopic LLL+HF calculations or experimental data. It is an effective low energy theory, so special care is needed to capture some physics at microscopic length scales

In this paper, we use both MCF approach and the CB approach developed in [12] to study spin polarized Tri-layer Quantum Hall (TLQH) systems at total filling factor $\nu_T = 1$. We also supplement the two approaches by wavefunction approach. TLQH is interesting from both experimental and theoretical sides. On the experimental side, TLQH systems have been fabricated in high mobility electron systems in the experimental group led by Shayegan [15]. On the theory side, because the three layers play the roles of three flavors. The excitons in BLQH is the pairing of particle in one layer and the hole in the other. This pairing structure in BLQH is similar to the Cooper pairing in BCS superconductors up to a particle-hole transformation. While the excitons in TLQH is not obvious, because so far there is no analog of three flavors superconductors yet. It would be interesting to understand the structures of the excitons and all the possible excitations in TLQH. As shown in this paper, due to the particular structure pattern of the excitons, there are two *coupled* Goldstone modes in the TLQH (see Eqn.33). In the presence of interlayer tunnelings (with or without in-plane magnetic field), the interference between the two gapless modes may also lead to many new phenomena which can not be seen in BLQH.

There are at least two well defined regimes for TLQH. (I) Interlayer coherent regime: when the distance d between the two adjacent layers is sufficiently small, then all the three layers are strongly correlated. (II) Weakly-coupled regime: when d is sufficiently large, then all the three layers are weakly coupled. Depending on the distance d , there could be many other possible regimes. In this paper, we focus on regime (I) which is the interlayer coherent regime. The system in the interlayer coherent regime (I) was discussed in [6,16] in LLL+ HF approach, two Goldstone modes are found. Here, we study the regime (I) in detail from both MCF and CB approaches and also stress the broken symmetry state in terms of $SU(3)$ algebra.

Consider a tri-layer system with N_1, N_2, N_3 electrons in layer 1 (the bottom layer), layer 2 (the middle layer) and layer 3 (the top layer) respectively in the presence of magnetic field $\vec{B} = \nabla \times \vec{A}$. We assume equal interlayer distance d between adjacent layers, the total filling factor is $\nu_T = 1$ and the spin is completely polarized. The Hamiltonian $H = H_0 + H_{int}$ is

$$H_0 = \int d^2x c_\alpha^\dagger(\vec{x}) \frac{(-i\hbar\vec{\nabla} + \frac{e}{c}\vec{A}(\vec{x}))^2}{2m} c_\alpha(\vec{x})$$

$$H_{int} = \frac{1}{2} \int d^2x d^2x' \delta\rho_\alpha(\vec{x}) V_{\alpha\beta}(\vec{x} - \vec{x}') \delta\rho_\beta(\vec{x}') \quad (1)$$

where electrons have bare mass m and carry charge $-e$; $c_\alpha, \delta\rho_\alpha(\vec{x}) = c_\alpha^\dagger(\vec{x})c_\alpha(\vec{x}) - \bar{\rho}_\alpha, \alpha = 1, 2, 3$ are electron

operators and normal ordered electron densities on the three layers. The intralayer interactions are $V_{11} = V_{22} = V_{33} = e^2/\epsilon r$, while interlayer interaction is $V_{12} = V_{21} = V_{23} = V_{32} = e^2/\epsilon\sqrt{r^2 + d^2}, V_{13} = V_{31} = e^2/\epsilon\sqrt{r^2 + 4d^2}$ where ϵ is the dielectric constant.

The rest of the paper is organized as follows. In section II, we discuss MCF approach to TLQH and point out its weakness. In section III, we discuss CB approach and derive an effective action involving the charge and the two Goldstone modes. We also derive a dual action of the CB approach and make critical comparisons between this dual action and the MCF action. We classify all the possible excitations and discuss possible 2-body and 3-body bound states and associated Kosterlize-Thouless transitions. In section IV, we will outline several salient features of correlated interlayer tunnelings with or without in-plane magnetic field in TLQH. We reach conclusions in the final section. At appropriate places in the paper, we point out the limitations of the CB approach.

II. MUTUAL COMPOSITE FERMION APPROACH:

We can extend the single-valued singular gauge transformation in [12] to tri-layer system:

$$U = e^{\frac{i}{2} \sum_{\alpha\beta} \int d^2x \int d^2x' U_{\alpha\beta} \rho_\alpha(\vec{x}) \arg(\vec{x} - \vec{x}') \rho_\beta(\vec{x}')} \quad (2)$$

where the 3×3 symmetric matrix U and its inverse is given by:

$$U_t = \begin{pmatrix} 0 & 1 & 1 \\ 1 & 0 & 1 \\ 1 & 1 & 0 \end{pmatrix} \quad U_t^{-1} = \frac{1}{2} \begin{pmatrix} -1 & 1 & 1 \\ 1 & -1 & 1 \\ 1 & 1 & -1 \end{pmatrix} \quad (3)$$

The Hamiltonian Eqn.1 is transformed into:

$$H_0 = \int d^2x \psi_\alpha^\dagger(\vec{x}) \frac{(-i\hbar\vec{\nabla} + \frac{e}{c}\vec{A}(\vec{x}) - \hbar\vec{a}_\alpha(\vec{x}))^2}{2m} \psi_\alpha(\vec{x}) \quad (4)$$

where the transformed fermion $\psi_\alpha(\vec{x}) = U c_\alpha(\vec{x}) U^{-1}$ is given by:

$$\psi_\alpha(\vec{x}) = e^{\frac{i}{2} \int d^2x' U_{\alpha\beta} [\arg(\vec{x} - \vec{x}') + \arg(\vec{x}' - \vec{x})] \rho_\beta(\vec{x}')} c_\alpha(\vec{x}) \quad (5)$$

and the three Chern-Simon (CS) gauge fields a_α in Eqn.4 satisfies: $\nabla \cdot \vec{a}_\alpha = 0, \nabla \times \vec{a}_\alpha = 2\pi U_{\alpha\beta} \rho_\beta(\vec{x}) = 2\pi[\rho(\vec{x}) - \rho_\alpha(\vec{x})]$ where $\rho(\vec{x}) = \sum_\alpha \rho_\alpha(\vec{x})$ is the total density of the system.

In the following, we put $\hbar = c = e = \epsilon = 1$. At total filling factor $\nu_T = 1$, $\nabla \times \vec{A} = 2\pi n$ where $n = n_1 + n_2 + n_3$ is the total average electron density. By absorbing the average values of CS gauge fields $\nabla \times \langle \vec{a}_\alpha \rangle = 2\pi(n - n_\alpha)$ into the external gauge potential $\vec{A}_\alpha^* = \vec{A} - \langle \vec{a}_\alpha \rangle$, we have:

$$H_0 = \int d^2x \psi_\alpha^\dagger(\vec{x}) \frac{(-i\vec{\nabla} + \vec{A}_\alpha^*(\vec{x}) - \delta\vec{a}_\alpha(\vec{x}))^2}{2m} \psi_\alpha(\vec{x}) \quad (6)$$

where $\nabla \times \vec{A}_\alpha^* = 2\pi n_\alpha$ and $\nabla \times \delta\vec{a}_\alpha = 2\pi U_{\alpha\beta} \delta\rho_\beta(\vec{x}) = 2\pi[\delta\rho(\vec{x}) - \delta\rho_\alpha(\vec{x})]$ are the deviations from the corresponding average density.

When $d < d_c/2$, the strong intra- and inter-layer interactions renormalize the bare mass into two different effective masses $m_1^* = m_3^*, m_2^*$ [14]. MCF in each layer feel effective magnetic field $B_\alpha^* = \nabla \times \vec{A}_\alpha^* = 2\pi n_\alpha$, therefore fill exactly one MCF Landau level. The energy gaps are simply the cyclotron gaps of the MCF Landau levels $\omega_{c\alpha}^* = \frac{B_\alpha^*}{m_\alpha^*}$.

Transport properties: Adding three different source gauge potentials \vec{A}_α^s to the three layers in Eqn.6, integrating out the MCF ψ_α first, then the mutual CS gauge fields, we can calculate the resistivity tensor by Kubo formula. We find that both Hall resistivity and two Hall drag resistivities are h/e^2 . This means if one drives current in one layer, the Hall resistivities in all the three layers are quantized at h/e^2 , while the longitudinal resistivities in all the three layers vanish. This is the hallmark of interlayer coherent quantum hall states.

In the following, we confine to balanced case $N_1 = N_2 = N_3 = N/3$, imbalanced case can be discussed along the similar line developed in [12].

Fractional charges: Let's look at the charge of quasi-particles created by MCF field operators $\psi_\alpha^\dagger(\vec{x})$. If we insert one electron at one of the layers, say layer 1, from the singular gauge transformation in Eqn.2, we can see this is equivalent to insert one MCF in layer 1, at the same time, insert one flux quantum at layer 2 and another one at layer 3 directly above the position where we inserted the electron. The inserted flux quantum at layer 2 and layer 3 are in the opposite direction to the external magnetic field, therefore promote one MCF in layer 2 and one in layer 3 to the second MCF Landau level in layer 2 and layer 3 respectively. Because inserting one electron leads to three MCFs in each layer, we conclude the charge of each MCF is $-1/3$. The above argument gives the correct *total* fractional charges of MCF, but it can not determine the *relative* charge distributions among the three layers. At mean field level, the energies of all the possible relative charge differences are degenerate. The lowest energy configuration can only be determined by fluctuations.

Left- and right-moving gapless modes: $\delta\rho_\alpha(\vec{x})$ can be expressed in terms of the CS gauge fields $\delta\rho_\alpha(\vec{x}) = [U_t^{-1}]_{\alpha\beta} \frac{\delta\vec{a}_\beta}{2\pi}$ where U_t^{-1} is given in Eqn.3. This constraint can be imposed by Lagrangian multipliers a_α^0 which plays the role of time components of CS gauge fields. Integrating out MCF ψ_1, ψ_2, ψ_3 to one-loop and carefully expanding the interlayer Coulomb interaction to the necessary order in the long-wavelength limit leads to an effective action for the three gauge fields.

$$\begin{aligned} \mathcal{L} = & \frac{iq}{4\pi} a_c^0 a_c^t + \frac{q}{16\pi} (a_c^t)^2 \\ & + \frac{\epsilon_c}{6} q^2 (a_c^0)^2 + \frac{1}{6} [\epsilon_c \omega^2 + (\chi_c - \frac{d}{3\pi}) q^2] (a_c^t)^2 \\ & + \frac{\epsilon_l}{4} q^2 (a_l^0)^2 + \frac{1}{4} [\epsilon_l \omega^2 + (\chi_l + \frac{d}{\pi}) q^2] (a_l^t)^2 \\ & + \frac{\epsilon_r}{12} q^2 (a_r^0)^2 + \frac{1}{12} [\epsilon_r \omega^2 + (\chi_r + \frac{d}{3\pi}) q^2] (a_r^t)^2 \\ & + \frac{\delta\epsilon}{9} q^2 a_c^0 a_r^0 + \frac{1}{9} [\delta\epsilon \omega^2 + (\delta\chi + \frac{d}{4\pi}) q^2] a_c^t a_r^t + \dots \quad (7) \end{aligned}$$

where $\vec{a}_s = \vec{a}_1 + \vec{a}_2 + \vec{a}_3$, $\vec{a}_l = \vec{a}_1 - \vec{a}_3$, $\vec{a}_r = \vec{a}_1 + \vec{a}_3 - 2\vec{a}_2$ which stand for center of mass, left and right channels respectively [17]. $\epsilon_c = (2\epsilon_1 + \epsilon_2)/3$, $\chi_c = (2\chi_1 + \chi_2)/3$, $\epsilon_l = \epsilon_1$, $\chi_l = \chi_1$, $\epsilon_r = (\epsilon_1 + 2\epsilon_2)/3$, $\chi_r = (\chi_1 + 2\chi_2)/3$, $\delta\epsilon = \epsilon_1 - \epsilon_2$, $\delta\chi = \chi_1 - \chi_2$. The dielectric constants $\epsilon_\alpha = \frac{m_\alpha^*}{2\pi B_\alpha^*}$ and the susceptibilities $\chi_\alpha = \frac{1}{2\pi m_\alpha^*}$ were calculated in single layer system in [18]. \dots are higher gradient terms and a_α^t is the transverse component of gauge fields in Coulomb gauge $\nabla \cdot \vec{a}_\alpha = 0$. The system is invariant under the Z_2 symmetry which exchanges layer 1 and 3, namely $a_c \rightarrow a_c, a_l \rightarrow -a_l, a_r \rightarrow a_r$. This symmetry dictates that only $a_c a_c, a_c a_r, a_r a_r, a_l a_l$ can appear in the Maxwell terms. The last two terms in Eqn. 7 which is the coupling between a_c and a_r can be shown to be irrelevant in the low energy limit.

More intuitive choices are $a_u = a_1 - a_2, a_d = a_2 - a_3$ which is related to a_l, a_r by $a_l = a_u + a_d, a_r = a_u - a_d$. But a_u and a_d are coupled, the two normal modes are a_l, a_r instead of a_u, a_d . As expected, there is a Chern-Simon term for the center of mass gauge field \vec{a}_s , while there are two Maxwell terms for the left and right channel gauge fields \vec{a}_l, \vec{a}_r which are gapless. The two gapless modes stand for the relative charge density fluctuations among the three layers. After putting back \hbar, c, e, ϵ , we find the two spin-wave velocities in terms of experimentally measurable parameters:

$$\begin{aligned} v_l^2 &= \frac{3(\omega_c^*)^2}{2\pi n} + \left(\frac{2\alpha c}{\epsilon}\right) \left(\frac{d}{l}\right) \frac{\omega_c^*}{\sqrt{2\pi n}} \\ v_r^2 &= \frac{3(\omega_c^*)^2}{2\pi n} \frac{1 + 2\gamma^{-1}}{1 + 2\gamma} + \left(\frac{2\alpha c}{\epsilon}\right) \left(\frac{d}{l}\right) \frac{\omega_c^*}{\sqrt{2\pi n}} \frac{1}{1 + 2\gamma} \quad (8) \end{aligned}$$

where we set $\omega_c^* = \omega_{c1}^*$ and n is the total density, l is the magnetic length, γ is the ratio of the two effective masses $\gamma = m_2^*/m_1^*$ and $\alpha \sim 1/137$ is the fine structure constant.

As in BLQH [12], we expect the second term dominates the first, then $v_l/v_r \sim \sqrt{1 + 2\gamma}$. namely, the ratio of the two velocities is determined by the ratio of the two effective masses. If we take the effective masses to be the band mass, then $v_l/v_r \sim \sqrt{3}$.

Topological excitations: As discussed in the previous paragraph, the MCF carries charge $1/3$, but their relative charge distributions among the three layers are undetermined. They can be characterized by their (a_c, a_l, a_r) charges $(\pm 1/3, q_l, q_r)$ with $q_l, q_r = 0, \pm 1, \dots$. Exchanging a_c leads to $1/r$ interaction between two MCF, while

exchanging a_l, a_r leads to logarithmic interactions which may lead to a 2-body bound state between two MCF with opposite (q_l, q_r) . The energy of this bound state with length L is $\Delta_+ + \Delta_- + q_c^2 \frac{e^2}{L} - (q_{l1}q_{l2} + \frac{q_{r1}q_{r2}}{1+2\gamma})\hbar\omega_c^* \ln L/l$ where Δ_+, Δ_- are the core energies of QH and QP respectively. There are also possible 3-body bound states of three MCF with $\sum_i q_{li} = \sum_i q_{ri} = 0$.

Unfortunately, the gluing conditions (or selection rules) of (q_c, q_l, q_r) for realizable physical excitations are not clear. This charge q_c and two spin (q_l, q_r) connections can only be easily established from CB approach presented in the next section. So we defer the discussion on the classification of all the possible excitations to the next section.

Problems with MCF approach:

All the criticisms on MCF approach to BLQH also hold to TLQH. In the following, we list just ones which are the most relevant to this paper.

(a) It is easy to see that the spin wave dispersion in Eqn.8 remains linear $\omega \sim vk$ even in the $d \rightarrow 0$ limit. This contradicts with the well established fact that in the $d \rightarrow 0$ limit, the linear dispersion relation will be replaced by quadratic $SU(3)$ Ferromagnetic spin-wave dispersion relation $\omega \sim k^2$ due to the enlarged $SU(3)$ symmetry at $d \rightarrow 0$.

(b) The broken symmetry in the ground state is not obvious without resorting to the $(111, 111)$ wavefunction Eqn.28. The origin of the gapless mode is not clear.

(c) The physical meaning of q_l, q_r is not clear. That they have to be integers was put in by hand in an ad hoc way.

(d) The spin-charge connections in (q_c, q_l, q_r) can not be extracted.

(e) Even in the balanced case, there are two MCF cyclotron gaps $\hbar\omega_{c\alpha}^*, \alpha = 1, 2$ at mean field theory. However, there is only one charge gap in the system. It is not known how to reconcile this discrepancy within MCF approach.

(f) In the presence of interlayer tunneling, it is not known how to derive the tunneling term in a straightforward way (see section IV).

In the following, we will show that the alternative CB approach not only achieve all the results, but also can get rid of all these drawbacks.

III. COMPOSITE BOSON APPROACH

Composite boson approach was found to be much more effective than the MCF approach in BLQH. We expect it remains true in TLQH. In this section, we apply CB approach to study TLQH and find that it indeed avoids all the problems suffered in MCF approach listed in the last section. Instead of integrating out the charge degree of freedoms which was done in the previous CB approach, we keep one charge sector and two spin sectors

on the same footing and explicitly stress the spin and charge connections. We classify all the possible excitations, bound states and associated KT transitions.

By defining the center of mass, left and right channels densities as:

$$\begin{aligned}\delta\rho_c &= \delta\rho_1 + \delta\rho_2 + \delta\rho_3 \\ \delta\rho_l &= \delta\rho_1 - \delta\rho_3 \\ \delta\rho_r &= \delta\rho_1 - 2\delta\rho_2 + \delta\rho_3\end{aligned}\quad (9)$$

We can rewrite H_{int} in Eqn.1 as:

$$\begin{aligned}H_{int} &= \frac{1}{2}\delta\rho_1 U \delta\rho_1 + \frac{1}{2}\delta\rho_2 U \delta\rho_2 + \frac{1}{2}\delta\rho_3 U \delta\rho_3 \\ &+ \delta\rho_1 V \delta\rho_2 + \delta\rho_2 V \delta\rho_3 + \delta\rho_1 W \delta\rho_3 \\ &= \frac{1}{2}\delta\rho_c V_c \delta\rho_c + \frac{1}{2}\delta\rho_l V_l \delta\rho_l + \frac{1}{2}\delta\rho_r V_r \delta\rho_r + \delta\rho_c V_{cr} \delta\rho_r\end{aligned}\quad (10)$$

where $U = V_{11}, V = V_{12}, W = V_{13}$ and $V_c = \frac{U}{3} + \frac{4V}{9} + \frac{2W}{9}, V_l = \frac{1}{2}(U - W), V_r = \frac{1}{3}(\frac{U}{2} - \frac{2V}{3} + \frac{W}{6}), V_{cr} = -\frac{1}{9}(V - W)$. The stability of the system dictates $V_c V_r - V_{cr}^2 > 0$. In the long wavelength limit $qd \ll 1$, we only keep the leading terms: $V_c = \frac{2\pi}{q}, V_l = 2\pi d, V_r = \frac{2\pi d}{9}, V_{cr} = -\frac{2\pi d}{9}$.

Performing a singular gauge transformation:

$$\phi_a(\vec{x}) = e^{i \int d^2 x' \arg(\vec{x} - \vec{x}') \rho(\vec{x}')} c_a(\vec{x}) \quad (11)$$

where $\rho(\vec{x}) = c_1^\dagger(\vec{x})c_1(\vec{x}) + c_2^\dagger(\vec{x})c_2(\vec{x}) + c_3^\dagger(\vec{x})c_3(\vec{x})$ is the total density of the tri-layer system.

After absorbing the external gauge potential \vec{A} into the Chern-Simon gauge potential \vec{a} , we can transform the Hamiltonian Eqn.1 into the Lagrangian in the Coulomb gauge:

$$\begin{aligned}\mathcal{L} &= \phi_a^\dagger(\partial_\tau - ia_0)\phi_a + \phi_a^\dagger(\vec{x}) \frac{(-i\hbar\vec{\nabla} - \hbar\vec{a}(\vec{x}))^2}{2m} \phi_a(\vec{x}) \\ &+ ia_0\bar{\rho} + \frac{1}{2} \int d^2 x' \delta\rho_c(\vec{x}) V_c(\vec{x} - \vec{x}') \delta\rho_c(\vec{x}') \\ &+ \frac{1}{2} \int d^2 x' \delta\rho_l(\vec{x}) V_l(\vec{x} - \vec{x}') \delta\rho_l(\vec{x}') \\ &+ \frac{1}{2} \int d^2 x' \delta\rho_r(\vec{x}) V_r(\vec{x} - \vec{x}') \delta\rho_r(\vec{x}') \\ &+ \int d^2 x' \delta\rho_c(\vec{x}) V_{cr}(\vec{x} - \vec{x}') \delta\rho_r(\vec{x}') - \frac{i}{2\pi} a_0 (\nabla \times \vec{a})\end{aligned}\quad (12)$$

In the Coulomb gauge, integrating out a_0 leads to the constraint: $\nabla \times \vec{a} = 2\pi(\phi_a^\dagger\phi_a - \bar{\rho})$.

It can be shown that $\phi_a(\vec{x})$ satisfies all the boson commutation relations. We write the three bosons in terms of magnitude and phase

$$\phi_a = \sqrt{\bar{\rho}_a + \delta\rho_a} e^{i\theta_a} \quad (13)$$

The boson commutation relations imply that $[\delta\rho_a(\vec{x}), \phi_b(\vec{x}')] = i\hbar\delta_{ab}\delta(\vec{x} - \vec{x}')$. For simplicity, in this paper, we only consider the balanced case, so we set

$\bar{\rho}_a = \bar{\rho}$. The imbalanced case can be discussed along similar lines developed in [12].

We define the center of mass, left-moving and right-moving angles which are conjugate angle variables to the three densities defined in Eqn.9

$$\begin{aligned}\theta_c &= \theta_1 + \theta_2 + \theta_3 \\ \theta_l &= \theta_1 - \theta_3 \\ \theta_r &= \theta_1 - 2\theta_2 + \theta_3\end{aligned}\quad (14)$$

which satisfy the commutation relations $[\delta\rho_\alpha(\vec{x}), \theta_\beta(\vec{x}')] = A_\alpha i\hbar\delta_{\alpha\beta}\delta(\vec{x} - \vec{x}')$ where $A = 3, 2, 6$ for $\alpha = c, l, r$.

Substituting Eqn.13 into Eqn.12, neglecting the magnitude fluctuations in the spatial gradient term which were shown to be irrelevant in BLQH in [12] and rewriting the spatial gradient term in terms of the three angles in Eqn.14, we find:

$$\begin{aligned}\mathcal{L} &= i\delta\rho_c(\frac{1}{3}\partial_\tau\theta_c - a_0) + \frac{\bar{\rho}}{2m}[\frac{1}{3}\nabla\theta_c - \vec{a}]^2 + \frac{1}{2}\delta\rho_c V_c(\vec{q})\delta\rho_c \\ &+ \frac{i}{2}\delta\rho_l\partial_\tau\theta_l + \frac{\bar{\rho}}{12m}(\nabla\theta_l)^2 + \frac{1}{2}\delta\rho_l V_l(\vec{q})\delta\rho_l \\ &+ \frac{i}{6}\delta\rho_r\partial_\tau\theta_r + \frac{\bar{\rho}}{36m}(\nabla\theta_r)^2 + \frac{1}{2}\delta\rho_r V_r(\vec{q})\delta\rho_r \\ &+ \delta\rho_c V_{cr}(\vec{q})\delta\rho_r - \frac{i}{2\pi}a_0(\nabla \times \vec{a})\end{aligned}\quad (15)$$

In the balanced case, the symmetry is $U(1)_c \times U(1)_l \times U(1)_r \times Z_2$ where the first is a local gauge symmetry, the second and the third are global symmetries and the global Z_2 symmetry is the exchange symmetry between layer 1 and layer 3.

(a) *Off-diagonal Algebraic order in the charge sector:*

At temperatures much lower than the vortex excitation energy, we can neglect vortex configurations in Eqn.15 and only consider the low energy spin-wave excitation. The charge sector (θ_c mode) and the two spin sectors (θ_l, θ_r modes) are essentially decoupled. It can be shown that the second to the last term $\delta\rho_c V_{cr}(\vec{q})\delta\rho_r$ in Eqn.15 which is the coupling between the charge sector and right-moving sector is irrelevant in the long wave-length limit. Therefore, the charge sector is essentially the same as the CSGL action in BLQH. Using the constraint $a_t = \frac{2\pi\delta\rho_c}{q}$, neglecting vortex excitations in the ground state and integrating out $\delta\rho_c$ leads to the effective action of θ_c :

$$\mathcal{L}_c = \frac{1}{2} \times (\frac{1}{3})^2 \theta_c(-\vec{q}, -\omega) [\frac{\omega^2 + \omega_q^2}{V_c(q) + \frac{4\pi^2\bar{\rho}}{m} \frac{1}{q^2}}] \theta_c(\vec{q}, \omega) \quad (16)$$

where $\omega_q^2 = \omega_c^2 + \frac{\bar{\rho}}{m}q^2 V_c(q)$ and $\omega_c = \frac{2\pi\bar{\rho}}{m}$ is the cyclotron frequency.

From Eqn.16, we can find the equal time correlator of θ_c :

$$\begin{aligned}\langle \theta_c(-\vec{q})\theta_c(\vec{q}) \rangle &= \int_{-\infty}^{\infty} \frac{d\omega}{2\pi} \langle \theta_c(-\vec{q}, -\omega)\theta_c(\vec{q}, \omega) \rangle \\ &= 3 \times \frac{2\pi}{q^2} + O(\frac{1}{q})\end{aligned}\quad (17)$$

which leads to the algebraic order:

$$\langle e^{i(\theta_c(\vec{x}) - \theta_c(\vec{y}))} \rangle = \frac{1}{|x - y|^3} \quad (18)$$

We could define $\tilde{\theta}_c = (\theta_1 + \theta_2 + \theta_3)/3 = \theta_c/3$, then the exponent will be $1/3$. But when we consider topological vortex excitations, then $e^{i\tilde{\theta}_c}$ may not be single valued. Therefore, θ_c is more fundamental than $\tilde{\theta}_c$.

(b) *Spin wave excitations:*

While in the spin sector, there are two neutral gapless modes: left-moving mode and right-moving mode [17]. Integrating out $\delta\rho_l$ leads to

$$\mathcal{L}_l = \frac{1}{2V_l(\vec{q})}(\frac{1}{2}\partial_\tau\theta_l)^2 + \frac{\bar{\rho}}{12m}(\nabla\theta_l)^2 \quad (19)$$

where the dispersion relation of spin wave can be extracted:

$$\omega^2 = [\frac{2\bar{\rho}}{3m}V_l(\vec{q})]q^2 = v_l^2 q^2 \quad (20)$$

In the long wave-length limit $qd \ll 1$, the bare spin wave velocity is:

$$v_l^2 = \frac{\bar{\rho}}{m} \frac{4\pi e^2}{3\epsilon} d = \frac{2e^2}{3m\epsilon} \sqrt{2\pi\bar{\rho}} \left(\frac{d}{l}\right) \quad (21)$$

Integrating out $\delta\rho_r$ leads to

$$\mathcal{L}_r = \frac{1}{2V_r(\vec{q})}(\frac{1}{6}\partial_\tau\theta_r)^2 + \frac{\bar{\rho}}{36m}(\nabla\theta_r)^2 \quad (22)$$

where the dispersion relation of spin wave can be extracted:

$$\omega^2 = [\frac{2\bar{\rho}}{m}V_r(\vec{q})]q^2 = v_r^2 q^2 \quad (23)$$

In the long wave-length limit $qd \ll 1$, the bare spin wave velocity is:

$$v_r^2 = \frac{\bar{\rho}}{m} \frac{4\pi e^2}{9\epsilon} d = v_l^2/3 \quad (24)$$

Both spin wave velocities should increase as the square root of the separation d when $d < d_c/2$, their ratio $v_l/v_r \sim \sqrt{3}$. At $d = 0$, $v_l = v_r = 0$. This is expected, because at $d = 0$ the $U(1)_l \times U(1)_r \times Z_2$ symmetry is enlarged to $SU(3)_G$, the spin wave of $SU(3)$ isotropic ferromagnet $\omega \sim k^2$.

We have also treated the coupling term between the charge and right-moving sector $\delta\rho_c V_{cr}(\vec{q})\delta\rho_r$ in Eqn.15 exactly and found that in the $\vec{q}, \omega \rightarrow 0$ limit, the mixed propagator takes the form:

$$\langle \theta_c(-\vec{q}, -\omega)\theta_r(\vec{q}, \omega) \rangle = \frac{\frac{9}{2}(\frac{m}{\pi\bar{\rho}})^2 V_{cr}\omega^2}{\omega^2 + v_r^2 q^2} \sim \omega^2 \langle \theta_r\theta_r \rangle \quad (25)$$

which is dictated by $\langle \theta_r \theta_r \rangle$ instead of $\langle \theta_c \theta_c \rangle$. Because of the ω^2 prefactor, we can ignore $\langle \theta_c \theta_r \rangle$ in the low energy limit.

We also found that Eqns.16, 17, 18 and Eqns.22,23,24 remain true in the long-wavelength and low energy limit, therefore confirm that $\delta \rho_c V_{cr}(\vec{q}) \delta \rho_r$ is indeed irrelevant in the limit.

As shown in BLQH in [12], the functional form of the spin sector in the CB theory is the same as EPQFM. Although there are no detailed microscopic calculations in TLQH yet except the preliminary work in [6,16], from the insights gained in BLQH, we can claim that the functional form of the spin sector in Eqn.15 (or Eqn.33) achieved in the CB theory is correct. Again, it is hard to incorporate the LLL projection in this CB approach, So some parameters can not be evaluated within this approach. For example, the two spin stiffnesses for the left and right-moving sectors in Eqn.15 (or or Eqn.33) should be completely determined by the Coulomb interactions instead of being dependent of the band mass, they may be estimated by the microscopic LLL+ HF approach. However, the ratio of the two velocities in Eqn.24 is independent of the band mass, it is interesting to see if this ratio $\sqrt{3}$ remains correct in the microscopic LLL+HF estimation. Just like in BLQH, we can simply take ρ_{sl}, V_l and ρ_{sr}, V_r in Eqn.15 as phenomenological parameters to be fitted into the LLL + HF estimations. However, just like in BLQH [10,12,19], because the qualitative correct ground state wavefunction in TLQH is still unknown, it is still difficult to estimate these parameters with controlled accuracy even in the LLL+HF approach. We can simply fit these parameters into experimental data.

(c) Dual action:

Just like in BLQH discussed in [12], we can perform a duality transformation on Eqn.15 to obtain a dual action in terms of three vortex currents $J_{\mu}^{v;c,l,r} = \frac{1}{2\pi} \epsilon_{\mu\nu\lambda} \partial_\nu \partial_\lambda \theta_{c,l,r}$ and three dual gauge fields $b_\mu^c, b_\mu^l, b_\mu^r$:

$$\begin{aligned} \mathcal{L}_d = & -i\pi b_\mu^c \epsilon_{\mu\nu\lambda} \partial_\nu b_\lambda^c - iA_{s\mu}^c \epsilon_{\mu\nu\lambda} \partial_\nu b_\lambda^c + i\frac{2\pi}{3} b_\mu^c J_\mu^{vc} \\ & + \frac{m}{2\bar{\rho}f} (\partial_\alpha b_0^c - \partial_0 b_\alpha^c)^2 + \frac{1}{2} (\nabla \times \vec{b}^c) V_c(\vec{q}) (\nabla \times \vec{b}^c) \\ & - iA_{s\mu}^l \epsilon_{\mu\nu\lambda} \partial_\nu b_\lambda^l + i\pi b_\mu^l J_\mu^{vl} \\ & + \frac{3m}{4\bar{\rho}} (\partial_\alpha b_0^l - \partial_0 b_\alpha^l)^2 + \frac{1}{2} (\nabla \times \vec{b}^l) V_l(\vec{q}) (\nabla \times \vec{b}^l) \\ & - iA_{s\mu}^r \epsilon_{\mu\nu\lambda} \partial_\nu b_\lambda^r + i\frac{\pi}{3} b_\mu^r J_\mu^{vr} \\ & + \frac{m}{4\bar{\rho}} (\partial_\alpha b_0^r - \partial_0 b_\alpha^r)^2 + \frac{1}{2} (\nabla \times \vec{b}^r) V_r(\vec{q}) (\nabla \times \vec{b}^r) \\ & + (\nabla \times \vec{b}^c) V_{cr}(\vec{q}) (\nabla \times \vec{b}^r) \end{aligned} \quad (26)$$

where the three source gauge fields are $A_{s\mu}^c = A_{1s\mu} + A_{2s\mu} + A_{3s\mu}$, $A_{s\mu}^l = A_{1s\mu} - A_{3s\mu}$, $A_{s\mu}^r = A_{1s\mu} - 2A_{2s\mu} + A_{3s\mu}$.

We can compare this dual action derived from CB ap-

proach with Eqn.7 derived in MCF approach. Just like in BLQH, the three topological vortex currents are missing in Eqn.7, while $\chi_c, \chi_l, \chi_r, \delta\chi$ terms are extra spurious terms which break $SU(3)$ symmetry even in the $d \rightarrow 0$ limit. If we drop all the χ terms, use bare mass and add the three vortex currents terms in Eqn.7, the resulting effective action will be identical to the dual action Eqn.26. Neglecting the vortex currents, we can identify the two spin wave velocities easily from the dual action which are the same as found previously from Eqn.15. It is also easy to show that the last term in Eqn.26 which is the coupling between the charge and right-moving sector is irrelevant in the low energy limit. We conclude that Eqns.15 and its dual action Eqn. 26 are the correct and complete effective actions.

(d) Topological excitations:

Any topological excitations are characterized by three winding numbers $\Delta\theta_1 = 2\pi m_1, \Delta\theta_2 = 2\pi m_2, \Delta\theta_3 = 2\pi m_3$, or equivalently, $\Delta\theta_c = 2\pi(m_1 + m_2 + m_3) = 2\pi m_c, \Delta\theta_l = 2\pi(m_1 - m_3) = 2\pi m_l, \Delta\theta_r = 2\pi(m_1 - 2m_2 + m_3) = 2\pi m_r$. It is important to stress that the three fundamental angles are $\theta_1, \theta_2, \theta_3$ instead of $\theta_c, \theta_l, \theta_r$. Therefore, m_1, m_2, m_3 are three independent integers, while m_c, m_l, m_r are not.

There are following 6 kinds of fundamental topological excitations: $\Delta\phi_1 = \pm 2\pi$ or $\Delta\phi_2 = \pm 2\pi$ or $\Delta\phi_3 = \pm 2\pi$, namely $(m_1, m_2, m_3) = (\pm 1, 0, 0), (0, \pm 1, 0), (0, 0, \pm 1)$. They correspond to inserting one flux quantum in layer 1 or 2 or 3 in the same or opposite direction as the external magnetic field. Let's classify the topological excitations in terms of (q, m_l, m_r) where q is the fractional charge of the topological excitations in the following table.

	$(\pm 1, 0, 0)$	$(0, \pm 1, 0)$	$(0, 0, \pm 1)$
m_c	± 1	± 1	± 1
m_l	± 1	0	∓ 1
m_r	± 1	∓ 2	± 1
q	$\pm 1/3$	$\pm 1/3$	$\pm 1/3$

Table 1: The fractional charge in balanced TLQH

The fractional charges in the table were determined from the constraint $\nabla \times \vec{a} = 2\pi\delta\rho_c$ and the finiteness of the energy in the charge sector:

$$q = \frac{1}{2\pi} \oint \vec{a} \cdot d\vec{l} = \frac{1}{2\pi} \times \frac{1}{3} \oint \nabla\theta_c \cdot d\vec{l} = \frac{1}{3} m_c \quad (27)$$

There are the following two possible bound states:

(1) Three Charge neutral two-body bound states:

- Layer 1: $(\pm 1/3, \pm 1, \pm 1)$ with energy $E_1 = E_{c+} + E_{c-} - \frac{e^2}{9R} + 2\pi(\rho_{sl} + \rho_{sr}) \ln \frac{R}{R_c}$ when $R \gg R_c \gg l$.
- Layer 2: $(\pm 1/3, 0, \mp 2)$ with energy $E_2 = E_{c+} + E_{c-} - \frac{e^2}{9R} + 2\pi(4\rho_{sr}) \ln \frac{R}{R_c}$.
- Layer 3: $(\pm 1/3, \mp 1, \pm 1)$ with energy $E_3 = E_1$ which is dictated by Z_2 symmetry.

The corresponding 2-body Kosterlize-Thouless (KT) transitions are $k_B T_{KT1}^{2b} = k_B T_{KT3}^{2b} = \frac{\pi}{2}(\rho_{sl} + \rho_{sr})$ which is dictated by Z_2 symmetry and $k_B T_{KT2}^{2b} = 2\pi\rho_{sr}$ above which the QP and QH pairs are liberated into free ones. If setting $\rho_{sl} = 3\rho_{sr}$, then there is only one 2-body KT temperature $k_B T_{KT}^{2b} = 2\pi\rho_{sr} = \frac{\pi\bar{\rho}}{9m}$. As explained previously, microscopic calculations in the LLL [22] are needed to estimate the two spin stiffnesses ρ_{sl} and ρ_{sr} . In general, there should be two 2-body KT transition temperatures $k_B T_{KT1}^{2b} = k_B T_{KT3}^{2b} \neq k_B T_{KT2}^{2b}$. The spin wave excitations will turn into these Charge neutral two-body bound states at large wavevector (or short distance). The two-body bound state behaves as a boson.

(1) Two Charge ± 1 three-body bound states:

The three-body bound states consists of three quasi-particles $(\pm 1/3, \pm 1, \pm 1)$, $(\pm 1/3, 0, \mp 2)$, $(\pm 1/3, \mp 1, \pm 1)$ located at the three corners of a triangle (Fig.1).

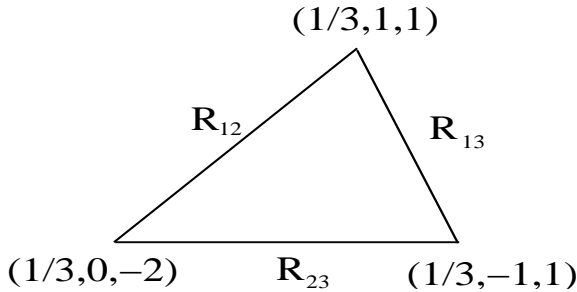


Fig 1: The lowest energy charged excitation is a three-body bound state of three $\pm 1/3$ charged quasi-particles sitting on the three corners of a triangle with $R_{12} = R_{23}$ dictated by the Z_2 symmetry. The three quantum numbers (q, m_l, m_r) are enclosed in the parenthesis

Its energy $E_{3b} = 3E_{c\pm} + \frac{e^2}{9}(\frac{1}{R_{12}} + \frac{1}{R_{23}} + \frac{1}{R_{13}}) + 2\pi[2\rho_{sr} \ln \frac{R_{12}}{R_c} + (\rho_{sl} - \rho_{sr}) \ln \frac{R_{13}}{R_c} + 2\rho_{sr} \ln \frac{R_{23}}{R_c}]$ when $R \gg R_c \gg l$. Minimizing E_{3b} with respect to R_{12}, R_{13}, R_{23} leads to two optimal separations: $R_{o12} = R_{o23} = \frac{e^2}{36\pi\rho_{sr}}$ which is dictated by the Z_2 symmetry and $R_{o13} = \frac{e^2}{18\pi(\rho_{lr} - \rho_{sr})}$. If setting $\rho_{sl} = 3\rho_{sr}$, then the three quasi-particles are located on the corners of a isosceles with length $R_o = \frac{e^2}{36\pi\rho_{sr}}$, the corresponding 3-body Kosterlize-Thouless (KT) transition is the same as the two-body bound state $k_B T_{KT}^{3b} = k_B T_{KT}^{2b} = 2\pi\rho_{sr} = \frac{\pi\bar{\rho}}{9m}$. These charged excitations behave as fermions and are the main sources of dissipations in transport experiments. In general, T_{KT}^{3b} should be different from the two 2-body KT transition temperatures. Again, microscopic calculations of the two spin stiffnesses ρ_{sl} and ρ_{sr} in the LLL [22] are needed to determine the three KT transition temperatures.

Let's look at the interesting possibility of deconfined (or free) $1/2$ charged excitations. Because any excitations with non-vanishing m_l or m_r will be confined, so any deconfined excitations must have $m_l = m_r = 0$ which

implies $m_1 = m_2 = m_3 = m$ and $m_c = 3m$. Eqn.27 implies the charge $q = \frac{1}{3}m_c = m$ must be an integer. This proof rigorously rules out the possibility of the existence of deconfined fractional charges. We conclude that *any deconfined charge must have an integral charge*. $m = 1$ corresponds to inserting one flux quantum through all the three layers which is conventional charge 1 excitation. Splitting the whole flux quantum into three fluxes penetrating the three layers at three different positions will turn into the three-body bound state with the same charge shown in Fig.1. It is still not known if the energy of this conventional charge 1 excitation is lower than the three body bound state.

IV. BROKEN SYMMETRY

The broken symmetry and associated Goldstone modes can be easily seen from wavefunction approach. In the first quantization, in the $d \rightarrow 0$ limit, the ground state trial wavefunction is the $(111, 111)$ state:

$$\Psi_{111,111} = \prod_{i=1}^{N_1} \prod_{j=1}^{N_2} (u_i - v_j) \prod_{i=1}^{N_1} \prod_{j=1}^{N_3} (u_i - w_j) \prod_{i=1}^{N_2} \prod_{j=1}^{N_3} (v_i - w_j) \times \prod_{i<j}^{N_1} (u_i - u_j) \prod_{i<j}^{N_2} (v_i - v_j) \prod_{i<j}^{N_3} (w_i - w_j) \quad (28)$$

where u, v, w are the coordinates in layer 1, 2 and 3 respectively.

In the second quantization, a trial wavefunction was written in [16]:

$$|\Psi\rangle = \prod_{m=0}^{M-1} \frac{1}{\sqrt{3}} (e^{i\theta_u} C_{m,1}^\dagger + C_{m,2}^\dagger + e^{i\theta_d} C_{m,3}^\dagger) |0\rangle = \prod_{m=0}^{M-1} \frac{1}{\sqrt{3}} (1 + e^{i\theta_u} C_{m,1}^\dagger C_{m,2} + e^{i\theta_d} C_{m,3}^\dagger C_{m,2}) \times \prod_{m=0}^{M-1} C_{m,2}^\dagger |0\rangle \quad (29)$$

where $\theta_u = \theta_1 - \theta_2, \theta_d = \theta_3 - \theta_2$ and $M = N$ is the angular momentum quantum number corresponding to the edge. We can interpret θ_u mode in Eqn.29 as a "up" pairing between an electron in layer 1 and a hole in layer 2 which leads to a θ_u molecule, similarly, θ_d mode as a "down" pairing between an electron in layer 3 and a hole in layer 2 which leads to a θ_d molecule (Fig. 2).

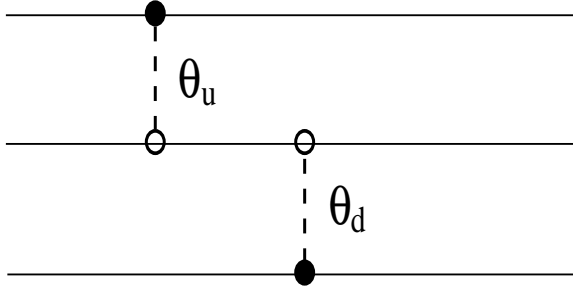


Fig 2: Two pairing modes of TLQH. Solid dots are electrons, open dots are holes.

Note that when $\theta_u = \theta_d = 0$, $|\Psi\rangle$ is the ground state $|G\rangle$, it can be shown [19] that its projection on (N_1, N_2, N_3) sector is $(111, 111)$ wavefunction in Eqn.28. Note that Eqn.28 is correct only in $d \rightarrow 0$ limit where the symmetry is enlarged to $SU(3)$. In the $SU(3)$ symmetric case, the pairing between any two layers of the three layers is equally likely. However, at any finite d , Eqn.28 and Eqn.29 may even not be qualitatively correct [19], because the $SU(3)$ symmetry is reduced to $U(1) \times U(1) \times U(1) \times Z_2$ symmetry (where the three $U(1)$ symmetry correspond to $c_\alpha(\vec{x}) \rightarrow e^{i\theta_\alpha} c_\alpha(\vec{x})$, $\alpha = 1, 2, 3$, $c_1 \leftrightarrow c_3$). The pairings between any two layers out of the three layers are not equivalent any more. The two lowest energy pairing modes are shown in Fig. 2.

$SU(3)$ has 8 generators which can be written in terms of c_α :

$$\begin{aligned} S_l(\vec{x}) &= c_1^\dagger(\vec{x})c_1(\vec{x}) - c_3^\dagger(\vec{x})c_3(\vec{x}) \\ S_r(\vec{x}) &= c_1^\dagger(\vec{x})c_1(\vec{x}) + c_3^\dagger(\vec{x})c_3(\vec{x}) - 2c_2^\dagger(\vec{x})c_2(\vec{x}) \\ S_{12}(\vec{x}) &= c_1^\dagger(\vec{x})c_2(\vec{x}), \quad S_{21}(\vec{x}) = S_{12}^\dagger(\vec{x}) = c_2^\dagger(\vec{x})c_1(\vec{x}) \\ S_{23}(\vec{x}) &= c_2^\dagger(\vec{x})c_3(\vec{x}), \quad S_{32}(\vec{x}) = S_{23}^\dagger(\vec{x}) = c_3^\dagger(\vec{x})c_2(\vec{x}) \\ S_{13}(\vec{x}) &= c_1^\dagger(\vec{x})c_3(\vec{x}), \quad S_{31}(\vec{x}) = S_{13}^\dagger(\vec{x}) = c_3^\dagger(\vec{x})c_1(\vec{x}) \end{aligned} \quad (30)$$

where S_l, S_r are the two (left and right) generators in Cartan subalgebra (Note that the algebra is *not* $SU(2)$ in spin $j = 1$ representation which is also 3 dimensional as used in [6]). In the balanced case $N_1 = N_2 = N_3 = N/3$, we have $\langle S_l \rangle = \langle S_r \rangle = 0$. The ground state in Eqn.28 breaks two of the three $U(1)$ symmetries, therefore there are two Goldstone modes in the corresponding two order parameters $\langle S_{12} \rangle = \frac{N}{3}e^{i\theta_u}$, $\langle S_{23} \rangle = \frac{N}{3}e^{-i\theta_d}$.

When θ_u molecule and θ_d molecule in Fig.2 move in the opposite direction, the currents in layer 2 cancel each other, it leads to the left-moving superfluid channel θ_l (Fig. 3a). While when θ_u molecule and θ_d molecule move in the same direction, the currents in layer 2 add and flow in the opposite direction to the currents in layer 1 and layer 3, it leads to the right-moving superfluid channel θ_r (Fig. 3b). In BLQH, there is only one superfluid channel which is the counter-flow channel [5]. In TLQH, there are two superfluid channels which are left-moving and right-moving channels, the left-moving channel corresponds to the counter-flow channel [17]. Obviously, it

is easier to perform transport experiments in the counter-flow channel than in the right-moving channel.

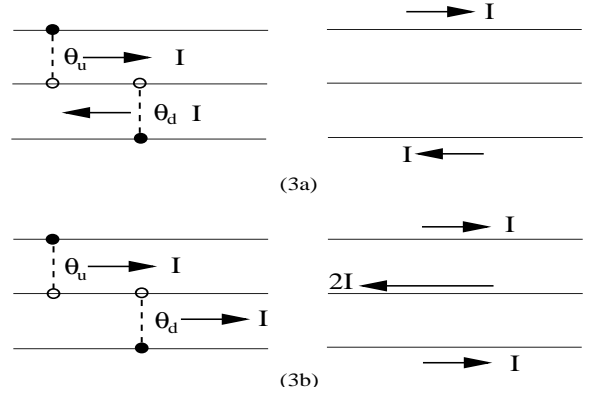


Fig 3: (3a) Left-moving superfluid channel which is the counter-flow channel (3b) Right-moving superfluid channel [17]

V. CORRELATED INTERLAYER TUNNELINGS

So far, we assume that the tunnelings are tuned to be zero. In this section, we will outline several salient features in the tunnelings of TLQH. We assume the tunneling amplitude from layer 1 to layer 2 is the same as that of from layer 2 to layer 3. The tunneling term is:

$$\begin{aligned} H_t &= tc_1^\dagger c_2 + h.c. + tc_2^\dagger c_3 + h.c. = t\phi_1^\dagger \phi_2 + h.c. + t\phi_2^\dagger \phi_3 + h.c. \\ &= t\bar{\rho}(\cos\theta_u + \cos\theta_d) = 2t\bar{\rho} \cos \frac{\theta_l}{2} \cos \frac{\theta_r}{2} \end{aligned} \quad (31)$$

where $\theta_u = \theta_1 - \theta_2$, $\theta_d = \theta_3 - \theta_2$

Integrating out the gapped charge sector θ_c leads to the effective tunneling action:

$$\begin{aligned} \mathcal{L} &= \frac{1}{2}[\chi_l(\partial_\tau \theta_l)^2 + \rho_{sl}(\nabla \theta_l)^2] + \frac{1}{2}[\chi_r(\partial_\tau \theta_r)^2 + \rho_{sr}(\nabla \theta_r)^2] \\ &\quad + 2t\bar{\rho} \cos \frac{\theta_l}{2} \cos \frac{\theta_r}{2} \end{aligned} \quad (32)$$

where, as noted previously, the two spin susceptibilities χ_l, χ_r and the two spin-stiffnesses ρ_{sl}, ρ_{sr} are phenomenological parameters to be fitted into the LLL+HF calculations or experimental data.

Unfortunately, the above action is not very useful for any practical calculations, because the two angles $\theta_l = \theta_u - \theta_d = \theta_1 - \theta_3$, $\theta_r = \theta_u + \theta_d = \theta_1 - 2\theta_2 + \theta_3$ are not independent angles when considering the vortex excitations. We can see this fact by noting that $\theta_l + \theta_r = 2\theta_u$ or $\theta_l - \theta_r = -2\theta_d$ has to be twice an angle which is a constraint between θ_l and θ_u . While θ_u and θ_d are two independent angles. So it is much more useful to write the above tunneling action in terms of the two independent angles θ_u, θ_d :

$$\begin{aligned}
\mathcal{L} = & \frac{1}{2}(\chi_l + \chi_r)(\partial_\tau \theta_u)^2 + \frac{1}{2}(\rho_{sl} + \rho_{sr})(\nabla \theta_u)^2 + t\bar{\rho} \cos \theta_u \\
& + \frac{1}{2}(\chi_l + \chi_r)(\partial_\tau \theta_d)^2 + \frac{1}{2}(\rho_{sl} + \rho_{sr})(\nabla \theta_d)^2 + t\bar{\rho} \cos \theta_d \\
& + (\chi_l - \chi_r)\partial_\tau \theta_u \partial_\tau \theta_d + (\rho_{sl} - \rho_{sr})\nabla \theta_u \cdot \nabla \theta_d \quad (33)
\end{aligned}$$

where there is a Z_2 symmetry under $\theta_u \leftrightarrow \theta_d$. The tunneling currents in three layers can be expressed in terms of the two independent angles: $I_1 = t\bar{\rho} \sin \theta_u$, $I_2 = -t\bar{\rho}(\sin \theta_u + \sin \theta_d)$, $I_3 = t\bar{\rho} \sin \theta_d$. They satisfy the current conservation $I_1 + I_2 + I_3 = 0$.

From Eqn.33, we can see there is a coupling between θ_u and θ_d . If there were not this coupling, we would have two independent BLQH tunneling actions. It is this coupling which lead to the *correlated* tunnelings of TLQH. For example, the current out of layer 1 $I_1 = t\bar{\rho} \sin \theta_u$ only depends on θ_u explicitly, while θ_u couples to θ_d . It was shown that the single gapless mode in BLQH leads to a sharp zero-bias peak in the interlayer tunneling of BLQH, the experimentally observed dissipations can only come from external sources such as disorder [21]. If the coupling in TLQH even in the absence of external sources will lead to a broad zero-bias tunneling peak in TLQH will be investigated in [22].

In the presence of in-plane magnetic field $B_{||} = (B_x, B_y)$, the gauge invariance dictates the tunneling term:

$$H_t = t\bar{\rho}(\cos(\theta_u - Q \cdot x) + \cos(\theta_d + Q \cdot x)) \quad (34)$$

where $Q_\alpha = (-\frac{2\pi dB_y}{\phi_0}, \frac{2\pi dB_x}{\phi_0})$.

In BLQH, it was found that the in-plane field will split the zero-bias peak, the splitting gives a direct measurement of the spin-wave velocity of the single Goldstone mode in BLQH [21]. However, in TLQH, there are two coupled Goldstone modes with two different velocities v_l, v_r . In [22], we will study how the zero-bias peak shifts and how to relate the shift to the two spin wave velocities or their ratio in the presence of in-plane magnetic field.

We can also see that if there were not the coupling between θ_u and θ_d , we would have two independent Pokrovsky-Talapov (PT) models. In BLQH which is described by a single PT model, it was found that when the applied in-plane magnetic field is larger than a critical field $B > B_{||}^*$, there is a phase transition from a commensurate state to an incommensurate state (C-IC) with broken translational symmetry. When $B > B_{||}^*$, there is a finite temperature KT transition which restores the translation symmetry by means of dislocations in the domain wall structure in the incommensurate phase [9,11]. In TLQH which is described by the above two coupled PT model [20], several kinds of C-IC transitions and associated several kinds of KT transitions are expected and will be studied in a separate publication [22].

VI. CONCLUSIONS:

In this paper, we study the interlayer coherent incompressible phase in spin polarized Trilayer Quantum Hall systems at total filling factor $\nu_T = 1$ from three approaches: MCF, CB and wavefunction approach. Just like in TLQH, CB approach is superior than MCF approach. The Hall and Hall drag resistivities are found to be quantized at h/e^2 . Two neutral gapless modes which are left and right moving modes with linear dispersion relations $v_{l/r} = \omega_{l/r}/k$ are identified and the ratio of the two velocities is close to $\sqrt{3}$. The novel excitation spectra are classified into two classes: (1) Charge neutral bosonic two-body bound states. (3) Charge ± 1 fermionic three-body bound states. In general, there are two 2-body KT transition temperatures and one 3-body KT transition temperature. Microscopic calculations in the LLL [22] are needed to roughly estimate the three KT transition temperatures. The Charge ± 1 three-body bound states shown in Fig. 1 may be the main dissipation source of the interlayer tunneling. The broken symmetry in terms of $SU(3)$ algebra is studied. The effective action of the two coupled Goldstone modes are derived. The excitonic structure in TLQH was shown in Fig. 2. In BLQH, there is only one superfluid channel which is the counter-flow channel [5]. In TLQH, there are two superfluid channels which are left-moving and right-moving channels (Fig.3), the left-moving channel corresponds to the counter-flow channel (Fig. 3a). Obviously, it is easier to perform transport experiments in the counter-flow channel than in the right-moving channel. In the presence of interlayer tunnelings, the coupling between the two Goldstone modes may lead to the broadening of the zero-bias tunneling peak, in contrast to the zero-bias peak in BLQH. The precise nature of the broadening and several other possible new phenomena unique to the TLQH in the presence of in-plane magnetic field will be studied in a forthcoming publication.

We expect that the effective action of the two coupled Goldstone modes and the qualitative physical pictures of TLQH achieved from CB approach in this paper are correct. However, the parameters in the effective action need to be estimated from microscopic calculations in the LLL [22]. It is interesting to see if the ratio $v_l/v_r \sim \sqrt{3}$ still holds in the microscopic calculations. As stressed in [10,19] for BLQH, the trial wavefunction Eqn.28 and Eqn.29 may not even be qualitatively correct in TLQH, so it is still difficult to estimate the ratio with controlled accuracy even in the LLL+HF approach. Eventually, the ratio need to be measured by experiments.

I thank J. K. Jain for helpful discussions.

- [1] B. I. Halperin, *Helv. Phys. Acta* 56, 75 (1983); *Surf. Sci.* 305, 1 (1994)
- [2] J. P. Eisenstein, L. N. Pfeiffer and K. W. West, *Phys. Rev. Lett.* 69, 3804 (1992); Song He, P. M. Platzman and B. I. Halperin, *Phys. Rev. Lett.* 71, 777 (1993).
- [3] I. B. Spielman *et al*, *Phys. Rev. Lett.* 84, 5808 (2000). *ibid*, 87, 036803 (2001).
- [4] M. Kellogg, *et al*, *Phys. Rev. Lett.* 88, 126804 (2002).
- [5] J.P. Eisenstein, A.H. MacDonald, cond-mat/0404113; M. Kellogg *et al*, cond-mat/0401521; E. Tutuc, M. Shayegan, D.A. Huse, cond-mat/0402186.
- [6] H. Fertig, *Phys. Rev. B* 40, 1087 (1989).
- [7] X. G. Wen and A. Zee, *Phys. Rev. Lett.* 69, 1811 (1992).
- [8] Z. F. Ezawa and A. Iwazaki, *Phys. Rev. B.* 48, 15189 (1993).
- [9] Kun Yang *et al*, *Phys. Rev. Lett.* 72, 732 (1994).
- [10] K. Moon *et al*, *Phys. Rev. B* 51, 5138 (1995).
- [11] For reviews of bilayer quantum Hall systems, see S. M. Girvin and A. H. Macdonald, in *Perspectives in Quantum Hall Effects*, edited by S. Das Sarma and Aron Pinczuk (Wiley, New York, 1997).
- [12] Jinwu Ye, cond-mat/0310512
- [13] Jinwu Ye, cond-mat/0407088
- [14] See the review by G. Murthy and R. Shankar, *Rev. of Mod. Phys.* 75, 1101, 2003.
- [15] J. Jo, Y. W. Suen, L. W. Engel, M. B. Santos, and M. Shayegan, *Phys. Rev. B* 46, 9776-9779 (1992); T. S. Lay, X. Ying, and M. Shayegan, *Phys. Rev. B* 52, R5511-5514 (1995).
- [16] C.B. Hanna and A.H. MacDonald, *Phys. Rev. B* 53 (23): 15981 (1996).
- [17] The "left" and "right" channels are used just to distinguish the two gapless channels. They have nothing to do with the moving directions in the real space.
- [18] A. Lopez and E. Fradkin, *Phys. Rev. B.* 44, 5246 (1991).
- [19] Gun Sang Jeon and Jinwu Ye, cond-mat/0407258. To appear in *Phys. Rev. B*.
- [20] This relation resembles that between Ising model and Ashkin-Teller model which is a model of two coupled Ising models.
- [21] L. Balents and L. Radzihovsky, *Phys. Rev. Lett.* 86, 1825 (2001). A. Stern, S. M. Girvin, A. H. Macdonald and N. Ma, *ibid* 86, 1829 (2001). M. Fogler and F. Wilczek, *ibid* 86, 1833 (2001).
- [22] Jinwu Ye, unpublished.